ATOMIC ENERGY OF CANADA LIMITED

THE DEPOSITION AND REMOVAL OF SUB-MICRON PARTICLES OF MAGNETITE AT THE SURFACE OF ALLOY 800

by

C.W. Turner, D.H. Lister and D.W. Smith

ABSTRACT

The rate of isothermal deposition of sub-micron particles of magnetite onto the surface of Alloy 800 has been measured at pHs between 4.2 and 9.3 at Re = 10 000 and a fluid temperature of 25°C. Deposition is modelled as a two-step process; transport of particles to the surface region followed by attachment to the surface. The deposition is limited by particle transport between pH 6.5 and 8.3, and by the rate of attachment for pH outside of this range. The rate of attachment has an Arrhenius dependence on surface temperature with an activation energy of 42 kJ/mole at pH 9.3. The rate of particle removal was negligible compared to the deposition rate, probably because the thickness of the viscous sub-layer was very much greater than the particle size.

System Chemistry and Corrosion Branch
AECL Research
Chalk River Laboratories
Chalk River, Ontario K0J 1J0 Canada

The Deposition and Removal of Sub-Micron Particles of Magnetite at the Surface of Alloy 800

C.W. Turner, D.H. Lister and D.W. Smith

1. INTRODUCTION

In nuclear steam generators, the accumulation of magnetite on tubes, tube support plates, and the tube sheet leads to a loss in heat transfer efficiency and to additional corrosion under the deposits. In order to minimize these deleterious effects, it is important to understand the mechanisms that govern the build-up of magnetite deposits under both heat transfer and isothermal conditions. The rate of deposition of particles onto a heat transfer surface depends on such parameters as the fluid velocity, fluid temperature, pH, particle size and mode of heat transfer. The effect of boiling heat transfer on the deposition rate should be determined under the steam generator operating conditions, whereas the effect of the other parameters can be determined at ambient temperature and extrapolated to operating conditions by taking account of the temperature dependence of the fluid properties.

Several studies of magnetite deposition have been reported in the literature. The most extensive study has been by Thomas [1] who examined the deposition of magnetite onto stainless steel tubes in the absence of heat transfer, as well as deposition with heat transfer in single and two-phase flow. All the experiments were done at neutral pH. For the isothermal experiments, Thomas correlated the results with the Reynolds number and found a logarithmic increase in the deposit mass per unit area with time for Re = 37 000 to 182 000 and an initial deposition rate that increased almost linearly with the Reynolds number. This suggests that eddy diffusion is the mechanism responsible for particle deposition in these experiments [2].

Gudmundsson reported the deposition rates of magnetite with an average particle size of 1.7 μm onto aluminum tubes at neutral pH for fluid temperatures ranging from 30 to 40°C and a Reynolds number ranging from 23 550 to 52 340 [3]. Gudmundsson found that the deposition rate increased by a factor of 2.5 when the fluid temperature was raised from 30 to 37°C and that the rate varied inversely with the fluid velocity. To explain this behaviour, Gudmundsson postulated a deposition rate with an exponential dependence on fluid temperature and which varied inversely with the friction velocity.

In subsequent work using the same apparatus as Gudmundsson, Newson [4] measured a deposition rate that increased with fluid velocity raised to the power 2.3. This is close to the rate dependence predicted for inertial coasting [2], but the magnitudes observed were 100 times lower than predicted by the theory. Newson et al.[5] continued the study of magnetite deposition on aluminum tubes in another experimental loop, but under similar experimental conditions as for the previous studies [3,4]. Their data showed the initial deposition rate increasing with fluid velocity raised to the power 0.5 to 1.0, which is in a range that is consistent with eddy diffusion.

Burrill examined the deposition behaviour of magnetite onto nickel and Zircaloy-4 tubes [6]. The isothermal experiments were conducted at 25°C, Re = 18 000 to 385 000, and pH = 4, 7, and 10. At pH = 7, Burrill found that for Re = 18 000 to 50 000, the deposition rate increased as Re^{6}, whereas for Re > 50 000 the deposition rate varied as $Re^{0.8}$. Burrill postulated that the deposition rate was controlled by inertial coasting at low Re and controlled by eddy diffusion at high Re.

Epstein has identified transport (mass transfer) and attachment (sticking, adhesion) as two sequential events in the fouling process [7]. Attachment is sometimes accounted for by multiplying the mass transfer rate by a sticking probability, which is defined as the probability that a particle that reaches the wall will stick to it. The sticking probability is usually given an Arrhenius dependence on the surface temperature and, in at least one case, an inverse-squared dependence on the fluid velocity [8]. Adhesion has since been put on a more fundamental basis by recognizing that when a particle arrives in the vicinity of the wall, its motion will be influenced by surface forces [9,10]. These forces include the van der Waals force of attraction as well as the force that arises from the overlap of the diffuse layers of charge associated with both the particle and the wall. The latter force is repulsive if the wall and particle have the same sign of surface charge. When the repulsive force is sufficiently large, there will be an activation energy which the particle must overcome if it is to reach the wall. Hence, the rate of attachment is equal to the rate at which particles surmount this energy barrier. The deposition rate is related to the rate of particle transport and the rate of particle attachment by:

$$K_d = (1/K_t + 1/K_a)^{-1}. \qquad \text{..... (1)}$$

This model has recently been applied to the deposition of silt onto a heated surface of stainless steel [11]. If the particle and wall are oppositely charged, then there is no surface repulsion and the deposition rate is determined solely by the rate of mass transfer to the wall.

Whether or not there is a repulsive force acting between the particle and the wall depends on the relative sign of their respective surface charges. The charge on each surface is a function of the pH. Hence, in order to model the deposition behaviour of particles onto a surface, it is necessary to determine the deposition rate as a function of pH and identify the pH ranges where deposition is transport- and attachment-limited, respectively. We report here the deposition behaviour of magnetite onto the surface of Alloy 800 at Re = 10 000 over the pH range 4.4 to 9.3.

2. EXPERIMENTAL METHODS AND ANALYSIS

The magnetite used for the deposition experiments was made by adding a 1.0 molar solution of potassium hydroxide to a solution that was 0.5 molar in both ferrous sulphate and potassium nitrate [12]. All solutions were prepared by adding reagent grade chemicals to distilled water that had been thoroughly purged with nitrogen. Following the addition of the hydroxide at room temperature to a final pH of 7.5, the mixture was aged for two hours at 90°C in a rotating round-bottomed flask and washed by decanting. The magnetite was examined by scanning electron microscopy (SEM) and transmission electron microscopy (TEM) to determine the particle size and morphology. The

sample was examined by x-ray diffraction and Mossbauer spectroscopy to confirm that the crystal phase was magnetite.

A schematic of the loop in which the deposition experiments were conducted is shown in Figure 1. The experiments were conducted under isothermal conditions at Re = 10 000. The fluid temperature was 25°C in all experiments but one, at pH = 9.3, where it was raised to 83°C. The 9.5 mm O.D. Alloy 800 test sections were sanded with 240, 360, and 600 grit emery paper in succession, to reduce the degree of surface roughness. Each test section was rinsed with hexane followed by methanol, to remove dirt and grease from the surface prior to being installed in the loop. The magnetite suspension was made 0.001 molar in potassium nitrate, to prevent large changes in ionic strength when the pH was adjusted between 4.4 and 9.3 by the addition of either nitric acid or potassium hydroxide. During the deposition phase, which typically lasted approximately 60 hours, the magnetite suspension was pumped from the suspension tank throughout the loop and samples were withdrawn from the loop periodically to determine the suspension pH, the magnetite concentration, and the magnetite electrophoretic mobility. The initial concentration of magnetite ranged from 10 to 25 mg/kg and the concentration generally decreased at the rate of 0.2%/h during the experiment. The decrease in magnetite concentration was accounted for in the calculation of the deposition rate. At the end of the deposition phase, the loop was flushed with water from the distilled water tank (see Figure 1) at the same ionic strength and pH as the magnetite suspension. The deposit mass was measured as a function of time (see below) in order to determine the rate of removal of magnetite by the fluid.

The mass of magnetite deposited per unit area was determined as a function of time by a radiotracing technique. A 0.5 g sample of magnetite was irradiated in the NRU reactor at Chalk River Laboratories to produce Fe-59 with a half-life of 44.5 days. The active magnetite was added to the loop make-up tank to a concentration of 3 mg/kg and mixed with the inactive magnetite. The activity of Fe-59 was determined on-line by measuring the intensity of the gamma ray at 1099 keV that signifies the decay of Fe-59 to Co-59. The on-line activity of the magnetite in suspension is related to the concentration of the magnetite in suspension by (symbols defined in the Nomenclature):

$$A_s = G\ C\ A\ \pi\ D^2\ L\ /\ 4, \quad \ldots\ldots\ldots\ldots\ldots\ldots \quad (2)$$

Similarly, the deposit activity is related to the deposit mass by:

$$A_d = G\ m\ A\ \pi\ D\ L, \quad \ldots\ldots\ldots\ldots\ldots\ldots \quad (3)$$

From Equations (2) and (3), the deposit mass per unit area is given by:

$$m = A_d\ (C/A_s)\ D\ /\ 4. \quad \ldots\ldots\ldots\ldots\ldots\ldots \quad (4)$$

Once the ratio C/A_s has been established (from a measurement at time zero), Equation (4) can be used to relate the deposit activity to the deposit mass at all subsequent times during the experiment.

At the end of each experiment, the absolute activity of the deposit on the test section was measured in an off-line counting facility in order to get an independent measurement of the deposit mass per unit area. The off-line and

on-line measurements of the deposit mass generally agreed to within 25%. Following the off-line measurement of the deposit activity, the test section was cut open and the deposit examined by scanning electron microscopy.

3. RESULTS AND DISCUSSION

An SEM micrograph of the magnetite particles prepared for this study is shown in Figure 2. A detailed examination of the particles by TEM suggested that they are formed from 0.01 μm crystallites by an agglomeration process during the aging step. The number-averaged diameter of the particles measured from a population of 175 particles was 0.26 $\pm$ 0.05 μm. Magnetite (Fe_3O_4) and maghemite (γ-Fe_2O_3) have face-centered cubic (fcc) and simple cubic (sc) crystal structures, respectively, with nearly identical unit cell sizes. Therefore, it is very difficult to distinguish between these two crystal phases from the positions of their x-ray diffraction lines. However, there are several low-angle reflections allowed in sc symmetry that are systematically absent in fcc symmetry. The comparison of observed and allowed x-ray reflections shown in Table 1 indicates that the sample prepared for this study was magnetite. However, as a further check on the crystal phase, the sample was examined by Mossbauer spectroscopy. The Mossbauer spectrum showed two sextuplets, corresponding to iron in tetrahedral and octahedral sites in the magnetite fcc lattice [13]. In contrast, the Mossbauer spectrum from maghemite would have shown only a single sextuplet.

Deposition rates were measured for 10 different pH values between 4.2 and 9.3. Figure 3 shows the deposit mass per unit area per unit suspension concentration as a function of time for selected values of the suspension pH. The deposition rate was lowest at pH 4.4. The rate increased steadily with increasing pH until the rate reached a maximum at pH 7.5. Further increases in pH caused the rate to decrease. Figure 3 also illustrates the general observation that the deposition rate decreased slowly with increasing time for the lower deposition rates, whereas the rate was constant with time for the higher deposition rates. A possible explanation for this is discussed later.

The data were analyzed to determine a deposition coefficient using the following equation:

$$m_d(t) = \rho\, K_d\, C\, t \qquad \text{..... (5)}$$

This analysis assumes that re-entrainment of the deposit during deposition is negligible. This assumption is shown to be valid in the discussion of the data on the removal rates given later. The deposition coefficient versus the suspension pH is shown in Figure 4. Where the rate decreased with time, the rate plotted is that at a deposition time of 5 hours. The deposition rate at pH 8.3 varied cyclically with time due to problems with controlling the loop pH. Hence, an average rate over 70 hours of deposition was used to calculate the deposition coefficient.

The information in Figure 4 was interpreted using a model that considers deposition to occur in two consecutive steps: transport of particles to the surface region followed by attachment of the particles to the surface. This model is expressed in mathematical form in Equation (1). The deposition rate will be limited by the rate of attachment over the pH range where magnetite

and Alloy 800 have the same sign of surface charge, and it will be limited by particle transport over the pH range where the surfaces of magnetite and Alloy 800 are oppositely charged. If it is assumed that the maximum deposition rate that occurs at pH 7.5 corresponds to the case where $K_a >> K_t$ (surfaces oppositely charged), the transport coefficient for 0.26 μm particles of magnetite in 25°C water at Re = 10 000 can be set equal to 3.5×10^{-7} m/s.

For the transport of particles to a surface under turbulent flow conditions, the rate of mass transfer is dominated by [2,14]:

i) eddy diffusion for $t_p^+ < 0.1$,
ii) inertial coasting for $0.1 < t_p^+ < 10$, and
iii) impaction for $t_p^+ > 10$.

The magnitude of t_p^+ was of order 10^{-4} for these experiments, hence eddy diffusion should govern the rate of particle transport to the surface. Cleaver and Yates [2] and Metzner and Friend [15], using entirely different approaches, calculated that the particle transport coefficient by eddy diffusion should be proportional to $U^* Sc^{-2/3}$ with a constant of proportionality of 0.084 and 0.0847, respectively. Hence, the theoretical transport coefficient for particles under the present conditions is equal to 8.7×10^{-7} m/s - 2.5 times the experimental value. We calculated deposition rates from Thomas' data [1] and found that they were, on average, a factor of two greater than the rates predicted for eddy diffusion. For this calculation, it was assumed that the magnetite agglomerates had been broken down to their constituent 0.05 μm particles by the fluid turbulence. The deposition rates reported by Newson et al.[5] were two to three times greater than the rates predicted for eddy diffusion. Note that the predicted rate is an upper limit (2) for smooth pipes, and that surface roughness will tend to enhance the transport of particles to the surface because of a decrease in the thickness of the viscous sublayer [14].

Figure 5 shows SEM micrographs of the magnetite particles deposited on a region of the test section that was 40 cm downstream from the inlet. The micrograph in Figure 5 (a) shows particles deposited at pH 9.3 and is typical of the deposit formed under conditions where the deposition rate was limited by the rate of attachment. The particles appear to deposit in clusters. Figure 5 (b) and (c) shows particles deposited at pH 7.5, where deposition was limited by particle transport to the surface. The regions of light and heavy deposit were at different locations around the circumference of the test section, and the pattern was repeated along the length of the test section. Surface roughness can affect the rate of particle transport, but the surface roughness does not appear to be different in the micrographs in Figure 5 (b) and (c). This pattern of deposition was only observed when the deposition rate was limited by particle transport.

Figure 6 shows the electrophoretic mobility of the magnetite added to the loop as a function of the loop suspension pH. Also shown is the estimated mobility-pH curve for Alloy 800, under the assumption that the surfaces of magnetite and Alloy 800 are oppositely charged near pH 7.5, where the deposition rate is a maximum. The fact that the deposition rate decreased somewhat between pH 7.5 and 8.3 implies that the surface of Alloy 800 must have a small, negative charge at the latter pH. Hence, the isoelectric point

(IEP) for Alloy 800 was estimated to occur at pH ~ 8. This is to be compared to an IEP between pH 3 and pH 4 for Types 304 and 347 stainless steel (16). For pH $\geq$ 8.3 and pH $\leq$ 6.5, where the surfaces of magnetite and Alloy 800 have the same sign of charge, the rate of attachment can be calculated from the measured deposition rate by substituting $K_t = 4.3 \times 10^{-7}$ m/s into Equation (1). From the magnitude of K_a at surface temperatures of 25 and 83°C, the activation energy for attachment at pH 9.3 was calculated to be 42 KJ/mole.

The rate at which magnetite was removed by the fluid during flushing (when release was measured) was negligible. Hence, the assumption that the rate of removal can be ignored for the analysis of the deposition data was justified. If the rate of deposit removal is proportional to the deposit mass, then:

$$m_r(t) = m_0 \exp(-\lambda t). \quad \ldots\ldots\ldots\ldots\ldots\ldots \quad (6)$$

The average value for λ in these experiments was 4×10^{-7} s^{-1}. From Equation (6), the time required to remove one half of the deposit by flushing would be 500 hours. For sub-micron particles in a steady flow, the drag force is proportional to the particle diameter squared and the lift force is zero [17]. Hence, steady flow does not provide a mechanism for removal of these particles from a surface. However, the viscous sub-layer is not steady, but there are sudden random eruptions of fluid, called turbulent bursts, that occur normal to the surface. Cleaver and Yates [18] argue that the updraft produced by the turbulent burst generates a small but finite lift force that, if sufficiently large, can be responsible for the removal of particles from a surface. For particles that are well submerged in the viscous sub-layer, the lift force generated by the turbulent burst will be rapidly dissipated by the viscous force [18], hence the rate of particle removal will be small. For the present experiments, the fact that the viscous sub-layer thickness of 62 μm was very much larger than the particle diameter is consistent with the very low rate of particle removal. From Cleaver and Yates' analysis [18]:

$$\lambda = U^{*2} f/100\nu, \quad \ldots\ldots\ldots\ldots\ldots\ldots \quad (7)$$

from which the constant, f, is equal to 7×10^{-9}. The constant, f, is a measure of the force of adhesion of the magnetite particles to the surface of Alloy 800. Having determined the magnitude of f, Equation (7) can now be used to predict removal rates for other thermalhydraulic conditions.

In contrast to a steady fluid flow past the deposit, a change in fluid velocity was considerably more effective at removing deposited particles. In several instances, between 5 and 15 percent (and in one case 70 percent) of the deposit was removed upon switching from deposition to removal, even though this operation resulted in no more than a 20% increase in fluid velocity, which lasted less than one minute before the controller brought the flow rate back to its set point. Typically, only five percent of the deposit would be removed during the subsequent 16 to 20 hours of steady operation. In experiments where the fluid velocity was increased step-wise during the release measurements to cover a three-fold range in fluid velocity, no systematic variation of λ with fluid velocity was observed. However, in some cases, between 25 and 75 percent of the deposit was removed at the instant that the flow rate was increased.

Figure 3 shows that the rate of deposit build-up decreased with increasing time for deposition limited by the rate of adhesion, and was constant for deposition that was transport limited. If the build-up of deposit was due to the simultaneous deposition and release of particles, then:

$$\frac{dm}{dt} = \rho K_d C - \lambda m, \quad \ldots\ldots\ldots\ldots\ldots\ldots\ldots \quad (8)$$

and,

$$m(t) = (\rho K_d C/\lambda)J(1 - \exp(-\lambda t)). \quad \ldots\ldots\ldots\ldots \quad (9)$$

For $\lambda = 7 \times 10^{-7}$ s^{-1}, Equation (9) predicts that the deposit mass will increase essentially linearly with time for the first 60 hours of deposition, which is consistent with the observed behaviour for transport-limited deposition. For attachment-limited deposition, the deviations from linearity occur within the first 10 hours of deposition, hence these deviations cannot be the result of a release mechanism. A possible explanation is that not all regions of the surface are at the same potential. Hence, deposition will occur first at regions of relatively low surface potential, i.e., regions of relatively low activation energy, at a higher rate of attachment. After these sites are occupied, deposition will continue at regions of higher surface potential, where the activation energy is higher and, consequently, the rate of attachment will be lower. These regions of varying surface potential might correspond to regions of varying thickness of the passive oxide film on Alloy 800. If this is the case, then Figure 5 (a) shows that the variation in the surface potential occurs on a scale of tens of microns.

4. SUMMARY

The rate of isothermal deposition of sub-micron particles of magnetite onto the surface of Alloy 800 has been measured over the pH range 4.2 to 9.3 at Re = 10 000 and a fluid temperature of 25°C. Deposition is modelled as a two-step process: transport of particles to the surface region followed by attachment to the surface. The deposition rate is limited by particle transport between pH 6.5 and 8.3, and is limited by the rate of attachment outside of this range. The rate of attachment has an Arrhenius dependence on surface temperature with an activation energy of 42 kJ/mole at pH 9.3. The rate of particle removal was negligible compared to the deposition rate, probably because the thickness of the viscous sub-layer was very much greater than the particle size.

5. NOMENCLATURE

A = absolute activity of magnetite (μC/g)
A_s = on-line suspension activity (c/s)
A_d = on-line deposit activity (c/s)
C = magnetite concentration (g/m^3)
D = test section I.D. (m)
E_a = activation energy (J/mole)
G = geometric factor relating absolute to measured activity
K_a = attachment coefficient = $K_o \exp(-E_a/RT_s)$ (m/s)
K_d = deposition coefficient (m/s)
K_t = transport coefficient (m/s)
K_o = pre-exponential constant

L = unit length of test section (m)
R = universal gas constant (J/mole K)
Re = Reynolds number = $u_m D/\nu$
Sc = Schmidt number = $3\pi\rho\nu^2 d/kT$
T = fluid temperature (K)
T_s = surface temperature (K)
U^* = friction velocity = $0.199\ u_m\ Re^{-1/8}$
d = particle diameter (m)
f = empirical constant
k = Boltzmann constant (J/K-mol)
m = deposit mass per unit area (g/m^2)
t = time (s)
t_p^+ = dimensionless relaxation time = $\frac{1}{18}\ \frac{\rho_p}{\rho}\ \frac{U^* d}{\nu}^2$
u_m = mean fluid velocity (m/s)
λ = removal time constant (s^{-1})
ρ = fluid density
ρ_p = particle density
ν = kinematic viscosity
δ = viscous sub-layer thickness = $5\nu/U^*$

6. REFERENCES

[1] D. Thomas and U. Grigull, "Experimental Investigation of the Deposition of Suspended Magnetite from the Fluid Flow in Steam Generating Boiler Tubes", Brennst.-Warme-Kraft, 26 (3) (1974) 109-117.

[2] J.W. Cleaver and B. Yates, "A Sub-layer Model for the Deposition of Particles from a Turbulent Flow", Chem. Eng. Sci. 30 (1975) 983-992.

[3] J. Gudmundsson, "Fouling of Surfaces", Ph.D. Thesis, University of Birmingham (1977).

[4] I.H. Newson, "Studies of Particulate Deposition from Flowing Suspension", Conference: Fouling - Science or Art? University of Surrey (1979).

[5] I.H. Newson, T.R. Bott, and C.I. Hussain, "Studies of Magnetite Deposition from a Flowing Suspension", ASME Heat Transfer Division Publication HTD V17, ASME, New York (1981) 73-81.

[6] K.A. Burrill, "The Deposition of Magnetite Particles from High Velocity Water onto Isothermal Tubes", Atomic Energy of Canada Limited Report AECL-5308 (1977).

[7] N. Epstein, "Thinking about Heat Transfer Fouling: a 5x5 Matrix", Heat Transfer Eng. 4 (1983) 43-56.

[8] P. Watkinson, "Particulate Fouling of Sensible Heat Exchangers", 4th Int. Heat Transfer Conf., Versailles, (1970)

[9] B.D. Bowen and N. Epstein, "Fine Particle Deposition in Smooth Parallel Plate Channels", J. Colloid and Interface Sci. 72 (1979) 81-97.

[10] E. Ruckenstein and D.C. Prieve, "Rate of Deposition of Brownian Particles under London and Double Layer Forces", J. Chem. Soc. Far. Trans. II 69 (1973) 1522-1536.

[11] C.W. Turner and D.H. Lister, "A Study of the Deposition of Silt onto the Surface of Type 304 Stainless Steel", Can. J. Chem. Eng., in press.

[12] T. Sugimoto and E. Matijevic, "Formation of Uniform Magnetite Particles by Crystallization from Ferrous Hydroxide Gels", J. Colloid and Interface Sci. 74 (1980) 227-243.

[13] N.N. Greenwood and T.C. Gibb, "Mossbauer Spectroscopy", Chapman and Hall, London, (1971).

[14] N. Epstein, "Particulate Fouling of Heat Transfer Surfaces: Mechanisms and Models", in Fouling Science and Technology, L.F. Melo, T.R. Bott, and C.A. Bernardo, eds., NATO ASI Series, Vol. 145, Kluwer Academic Publishers, Dordrecht (1988) p. 143.

[15] A.B. Metzner and W.L. Friend, "Theoretical Analogies Between Heat, Mass, and Momentum Transfer and Modifications for Fluids of High Prandtl or Schmidt Numbers", Can. J. Chem. Eng. 36 (1958) 235-240.

[16] B. Levy and A.R. Fritsch, Electrokinetic Measurements on Stainless Steel Capillaries", J. Electrochem. Soc. 106 (1959) 730-735.

[17] M.E. O'Neill, "A Sphere in Contact with a Plane Wall in a Slow Linear Shear Flow", Chem. Eng. Sci. 23 (1968) 1293-1298.

[18] J.W. Cleaver and B. Yates, "The Effect of Re-entrainment on Particle Deposition", Chem. Eng. Sci. 31 (1976) 147-151.

[19] Joint Committee on Powder Diffraction Standards (JCPDS) International Centre for Diffraction Data (1989).

TABLE 1: A comparison of the measured d-spacings and x-ray intensities for the magnetite prepared for this study with literature values for magnetite and maghemite (19).

d-spacing (nm)	relative intensity		
	magnetite	maghemite	sample
0.59	-	5	-
0.48	8	4	9
0.37	-	5	-
0.34	-	5	-
0.30	30	35	34
0.25	100	100	100

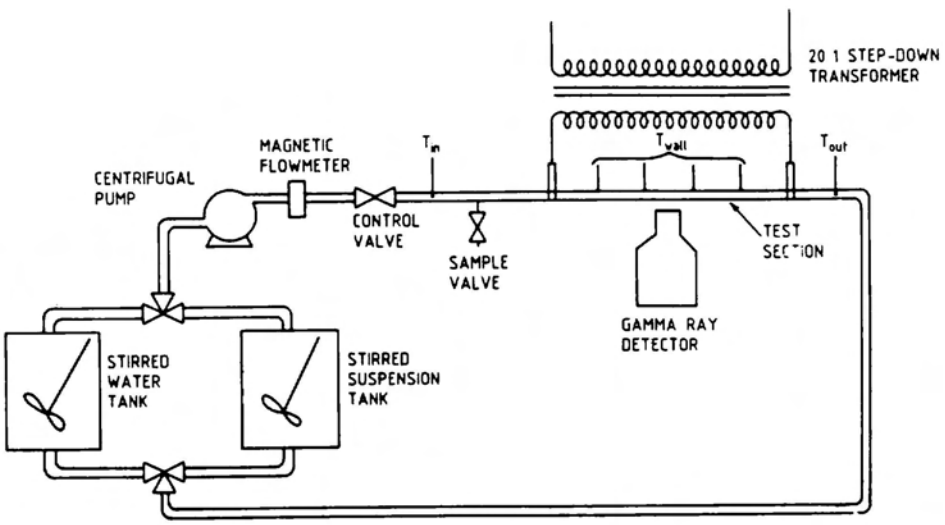

FIGURE 1: Schematic of the fouling ring.

FIGURE 2: An SEM micrograph of the magnetite particles used in the deposition experiments.

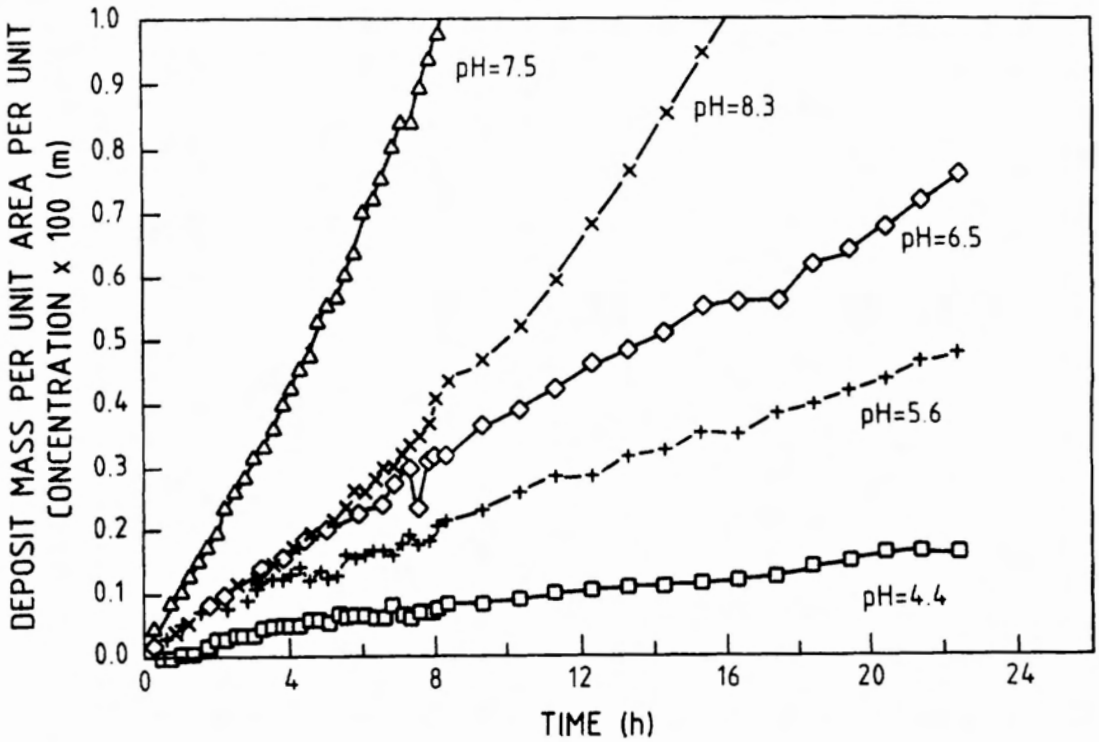

FIGURE 3: Deposit mass per unit area per unit concentration as a function of time for pH = 4.4 ( ), 5.6 (+), 6.5 ( ), 7.5 (Δ) and 8.3 (x).

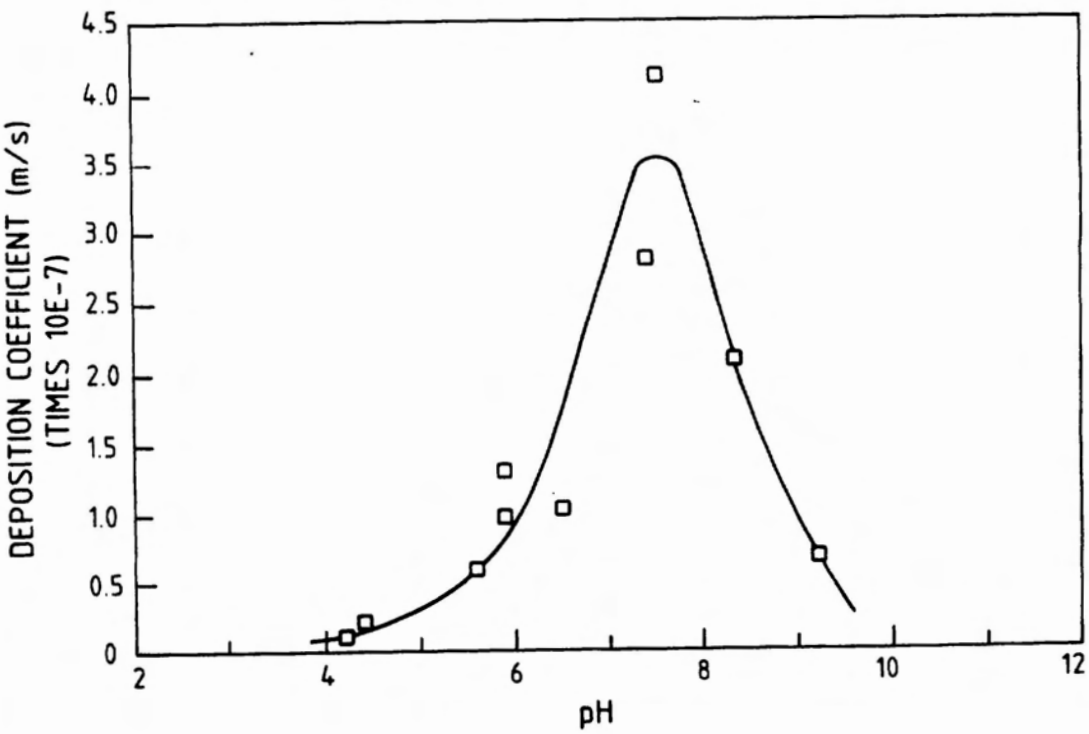

FIGURE 4: Deposition coefficient versus pH.

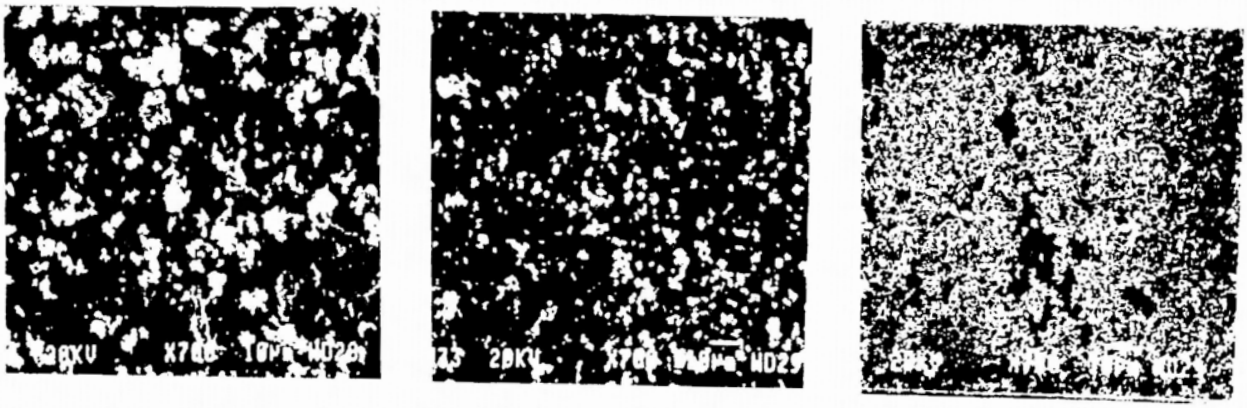

(a) (b) (c)

FIGURE 5: SEM micrographs of particles deposited at pH 9.3 (a) and 7.5 (b,c).

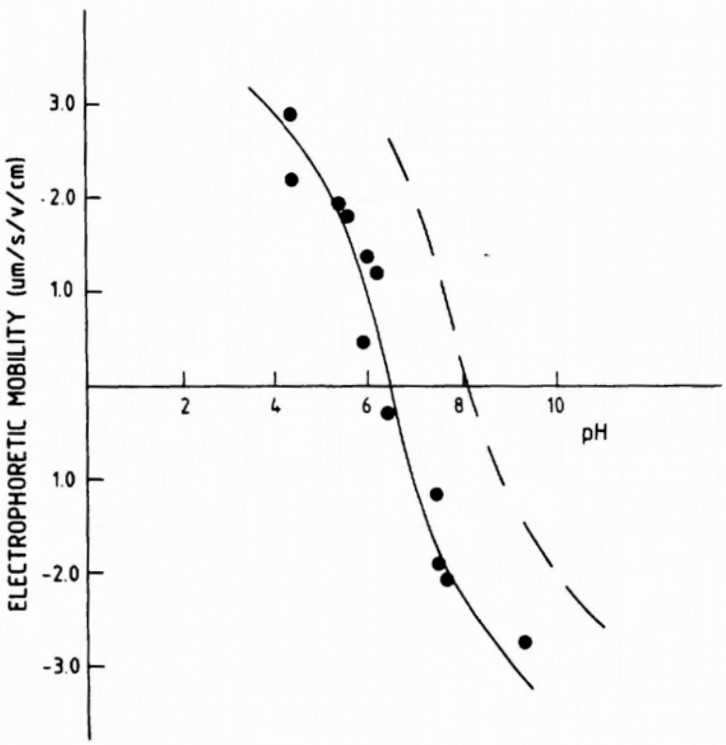

FIGURE 6: Electrophoretic mobility of magnetite ( ) and Alloy 800 (--) versus pH.